

RESEARCH

Open Access



Transfer Lengths in Pretensioned Concrete Measured Using Various Sensing Technologies

Se-Jin Jeon^{1*} , Ho Shin², Sang-Hyun Kim³, Sung Yong Park³ and Jun-Mo Yang⁴

Abstract

Although pretensioned concrete structures have increasingly been used worldwide, a number of design issues need to be addressed to further improve the structural performance. Transfer length of pretensioned members was investigated with several test variables in this study by adopting various sensing technologies including the Smart Strands with embedded fiber optic sensors. The effect of increased strength in 2360 MPa high-strength strand on the transfer length was also analyzed. Representative provisions widely used in design were compared with the test results for consistency and appropriate conservatism. The strain distribution required for the transfer length depended partly on the type and location of sensors, which suggests the challenges associated with reasonable determination of the transfer length. According to the results of the analysis, the predictive equation in ACI 318 was relatively accurate and conservative under various conditions including high-strength strands. However, the transfer lengths based on the strand strains rather than the conventional surface strains of concrete require further investigation depending on the bonding behavior between the strand and the surrounding concrete inside a member. Thus, this study also introduces a new sensing technology utilizing the Smart Strand to reliably measure the strain distribution along a strand.

Keywords: pretension, transfer length, transmission length, prestressing tendon, strand, prestressed concrete, fiber optic sensor

1 Introduction

Prestressed concrete (PSC) has been used to effectively overcome the low tensile strength and cracks in reinforced concrete by introducing compressive stress using prestressing tendons in advance. The PSC structures can be classified into two types including pretensioned and post-tensioned concrete. In the pretension method, after introducing tension force into the tendons arranged between the bulk-heads that are located at the ends of a pretensioning bed, concrete is cast into the form. When the concrete strength attains a certain level, the tendons are cut to introduce prestress into the concrete depending on the bonding behavior between the tendons and concrete. Seven-wire steel strands have been widely used as prestressing tendons (ASTM 2018; KATS 2018).

Based on the foregoing characteristics, no frictional loss of prestress occurs in the pretensioned concrete, which is one of the beneficial aspects when compared to post-tensioned concrete (Huang and Kang 2018). On the other hand, precast concrete structures have recently become increasingly popular worldwide due to a number of advantages that can be expected from systematic quality control during fabrication and assembly of precast members at a construction site. Accelerated and safe construction, high quality and durability, aesthetics, and other features of precast concrete overcome the drawbacks of conventional cast-in-place concrete structures. The precast concrete can be efficiently combined with pretension method in a large plant yard appropriate for mass production.

In the pretensioned concrete, several design issues can be traced to the pretensioning technique. Among these issues, transfer length (also called transmission length) is directly related to the distribution of prestressing force. The transfer length in a pretensioned member is defined by the length of embedded pretensioned strand

*Correspondence: conc@ajou.ac.kr

¹ Department of Civil Systems Engineering, Ajou University, 206, Worldcup-ro, Yeongtong-gu, Suwon-si, Gyeonggi-do 16499, Republic of Korea

Full list of author information is available at the end of the article
Journal information: ISSN 1976-0485 / eISSN 2234-1315

required to transfer the effective prestress to concrete by bond (ACI Committee 318 2019), which is measured from the end of the strand to the point where the effective prestress is developed. Therefore, the transfer length has a significant effect on the prestress distribution especially at the end region of a pretensioned member, which is comparable to the slip loss of prestress in a post-tensioned member (Hayek and Kang 2017). Extensive studies on the transfer lengths suggested the role of multiple factors in design codes and specifications (AASHTO 2017; ACI Committee 318 2019; BSI 1997; CEN 2004; fib 2013; KCI 2012; KRTA 2010, 2015; PCI 2017). However, the predictive equations of the transfer length show a wide variation depending on the provisions, which suggests the difficulty and uncertainty associated with the determination and evaluation of the variables affecting transfer length. Furthermore, because the transfer length largely depends on the strain distribution in a member, the sensor type and location has a significant effect on the transfer length under experimental conditions. However, systematic comparison of the transfer lengths based on the strains in different types of sensors has been very limited until now. On the other hand, strands with the ultimate tensile strength of 2360 MPa (KATS 2018; Kim et al. 2016b) have recently been developed to enhance structural and economic efficiency of PSC structures and to comply with the development and application of high-strength concrete. Extensive application of the high-strength strands requires adaptation or validation of current design equations including the transfer length originally developed for normal-strength strands (ASTM 2018; KATS 2018). Ultimate tensile strength of the strands most widely used at present is 1860 MPa.

Reflecting the foregoing state-of-the-art developments and trends, the transfer length of pretensioned members was investigated with several test variables in this study using sensing technologies such as the Smart Strands with embedded fiber optic sensors (KICT 2013; Kim et al. 2015). The effect of increased strength in 2360 MPa high-strength strand on the transfer length was also analyzed. Several representative provisions widely used in design were compared with the test results for consistency and conservatism.

2 Transfer Lengths in Provisions and Previous Studies

A prestressing tendon can be anchored inside concrete depending on the bond between the tendon and concrete combined with Hoyer effect during the tendon release from bulk-heads of a pretensioning bed. The Hoyer effect suggests deformation of the end of a tendon into a wedge-like shape depending on the Poisson's ratio (Briere et al. 2013). According to previous studies, several dominant

parameters including the diameter and surface conditions of a tendon, prestressing force, concrete strength, and speed of transfer at release affect the transfer length.

Russell and Burns (1996) investigated transfer length using the variables such as diameter, spacing, and number of strands, cross-sectional size of a rectangular member, partial debonding, and confining transverse reinforcements. They used demountable mechanical strain gauges (DEMEC gauges) to measure the strain distribution on the concrete surface. Even though electrical resistance strain gauges (ERSGs) mounted on the strand surface were used, these data were unreliable for the analysis of transfer length. Several drawbacks of the ERSGs applied for strand strain were addressed. As a result, a predictive equation was proposed similar to that of ACI 318 (ACI Committee 318 2019) and was adjusted to be more conservative.

Oh and Kim (2000) also utilized the DEMEC gauges to verify the existing predictive equations in terms of diameter, spacing, and number of strands as well as concrete cover and strength. Although they facilitated the determination of strains at strand surface using ERSGs, they were not used to determine the transfer length possibly due to the lack of reliability and were only used to partly validate the concrete strains.

Park (2015) performed the tests with the variables including diameter, spacing, and stress of strands, cross-sectional size of a rectangular member, concrete cover and strength, partial debonding, spacing of longitudinal reinforcements, and curing conditions. Based on the result, a predictive equation for transfer length was proposed by formulating bond characteristics. DEMEC gauges and ERSGs for both the concrete and strand strain were used for measurement, and the performance of the gauges was compared with each other.

Kim et al. (2016b) evaluated the transfer length based on the measurement of concrete surface strain using ERSGs. Although they also obtained data from DEMEC gauges, the data were not used due to low reliability. The variables analyzed were strand stress, concrete strength, confining transverse reinforcements, and volume fraction of fibers in concrete.

Provisions for transfer length involved in a variety of design codes and specifications are shown in Table 1. They show differences in parameters considered and the level of complexity. The simplest form of transfer length is found in AASHTO LRFD (AASHTO 2017) and the Korean design code for highway bridges (KDCHB) (KRTA 2010, 2015), which is defined only as a function of tendon diameter. The ACI 318-19 equation (ACI Committee 318 2019) is based on the equilibrium condition of a strand segment in the zone of transfer length assuming constant bond stress. The Korean structural

Table 1 Provisions for transfer length (unit: mm).

Provisions	Abbreviation	Predictive equation	Remarks
AASHTO LRFD (AASHTO 2017)	AASHTO	$60d_b$	d_b : strand diameter (mm)
KDCHB2 (KRTA 2015)	KDCHB2		
KDCHB1 (KRTA 2010)	KDCHB1	$50d_b$	d_b : strand diameter (mm)
ACI 318-19 (ACI Committee 318 2019)	ACI	$\frac{f_{se}d_b}{21}$	d_b : strand diameter (mm) f_{se} : effective prestress of strand (MPa)
PCI (PCI 2017)	PCI		
KSCDC (KCI 2012)	KSCDC		
BS 8110 (BSI 1997)	BS	$\frac{K_t\phi}{\sqrt{f_{ci}}}$	K_t : coefficient for tendon surface condition ϕ : tendon diameter (mm) f_{ci} : concrete strength at transfer (MPa)
Eurocode 2 (CEN 2004)	EC	$\frac{\alpha_1\alpha_2\phi\sigma_{pm0}}{f_{bpt}}$	α_1 : coefficient for speed of transfer α_2 : coefficient for tendon surface condition ϕ : tendon diameter (mm) σ_{pm0} : tendon stress upon transfer (MPa) f_{bpt} : bond stress (MPa)

concrete design code (KSCDC) (KCI 2012) and PCI (PCI 2017) also adhered to the transfer length of ACI 318-19. Therefore, AASHTO LRFD and KDCHB assumed a specific degree of tendon prestress in ACI 318-19 for simplification. BS 8110 (BSI 1997) incorporates additional parameters such as the surface condition of tendon and concrete strength but ignores the effect of tendon stress when compared to ACI 318-19. Eurocode 2 (CEN 2004) exhibits the most complicated form among the equations listed in Table 1. It considers the speed of transfer and bond stress in addition to surface condition, diameter, and stress of tendon. The bond stress is defined as a function of a few factors including concrete strength. The equation of fib (fib 2013) is even more complicated than that of Eurocode 2, although it is not presented in Table 1.

3 Fabrication of Specimens and Measurement Plan

3.1 Test Variables

The test variables were established based on a number of previous studies, including those introduced in chapter 2, and depending on the study goals including investigation of the structural behavior of high-strength strands. The variables included diameter, center-to-center spacing, and stress of strands, concrete strength, and speed of transfer. A few variables investigated in previous studies were less dominant from a practical perspective, and therefore, excluded or set to a single value in this study. Two specimens per variable were included to reduce any bias caused by a single specimen.

The center-to-center spacing of double strands was determined depending on the minimum center-to-center spacing of strands specified in various provisions (AASHTO 2017; ACI Committee 318 2019; KRTA 2010, 2015), which is 1.33 times the maximum size of aggregate

and 45 mm to 50 mm (for the strand diameter of 12.7 mm to 15.2 mm, respectively), and frequently used the range of 50–65 mm. The strands were tensioned up to $0.75f_{pu}$ considering the maximum permissible stress of $0.80f_{pu}$ and $0.94f_{py}$ (ACI Committee 318 2019; KCI 2012; KRTA 2010), where f_{pu} represents the ultimate tensile strength and f_{py} denotes the yield strength of strand. The final stress converged to $0.64f_{pu}$ on average after the slip loss occurring at the anchorages of the pretensioning bed. The actual compressive strengths of concrete at transfer after a certain period of curing were 31, 41, and 55 MPa for the specified compressive strengths of 35, 50, and 80 MPa, respectively, which complied with the minimum compressive strength of 30 MPa and 1.7 times the concrete stress required at transfer of a pretensioned member (KRTA 2010).

Figure 1 illustrates identification of a sample specimen depending on the variables. Table 2 presents the list of specimens expressed by this identification. Smart Strands were selectively applied for the measurement as described in the following section.

Figure 2 shows the cross sections of two representative specimens among 26 specimens in total. The specimens were fabricated in a rectangular shape as reported in most of the previous studies, and the concrete cover was set to approximately 50 mm or greater because the covers in this range showed negligible effect on the transfer length (Oh and Kim 2000; Park 2015). In fact, most of the pretensioned members such as pretensioned girders measure at least 50 mm in cover depth. The cover also complies with the minimum concrete cover of 30 mm (ACI Committee 318 2019) or 40 mm (KRTA 2010) required for the prestressing tendons used in this study. The length of all the specimens was 3000 mm, which was sufficient to determine the transfer lengths at both

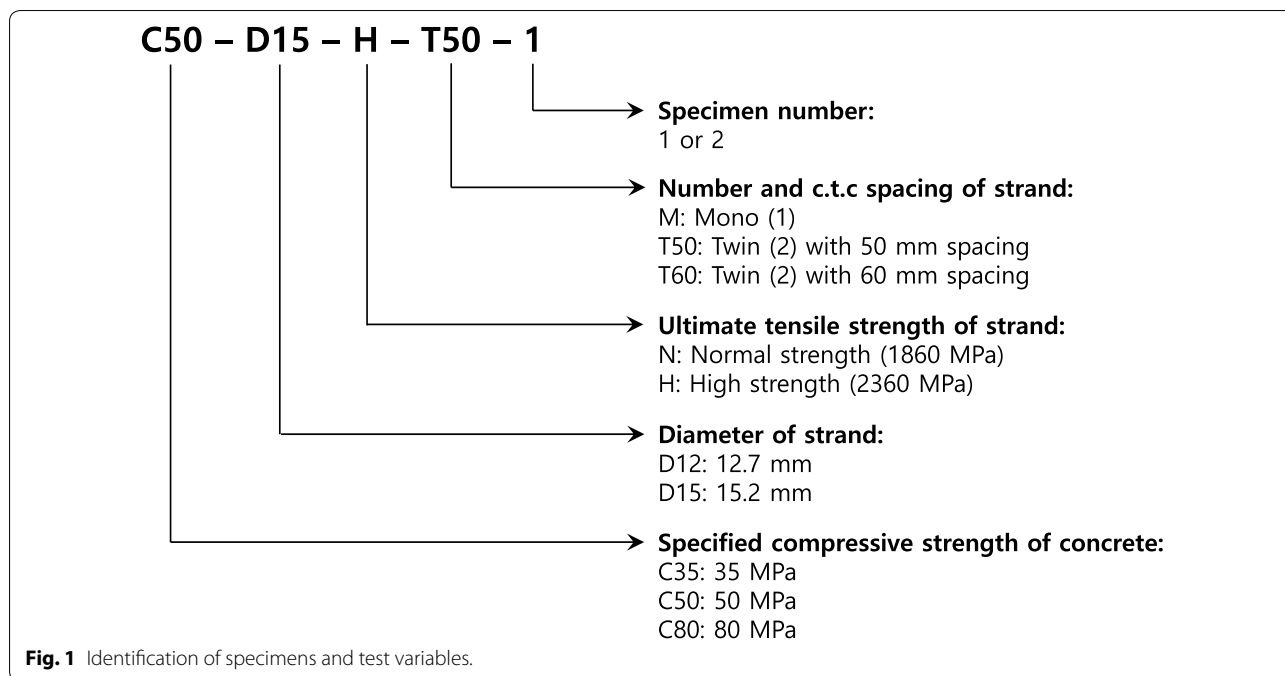


Table 2 List of specimens.

Series				Specimens		
M	C35	N	D12	C35-D12-N-M-1 C35-D12-N-M-2		
			D15	C35-D15-N-M-1 ^a C35-D15-N-M-2 ^a		
		H	D15	C35-D15-H-M-1 ^a C35-D15-H-M-2 ^a		
			C50	N	D12	C50-D12-N-M-1 C50-D12-N-M-2
		D15			C50-D15-N-M-1 ^b C50-D15-N-M-2 ^b	
		H	D15	C50-D15-H-M-1 ^b C50-D15-H-M-2 ^b		
	C80		N	D12	C80-D12-N-M-1 C80-D12-N-M-2	
		D15		C80-D15-N-M-1 ^a C80-D15-N-M-2 ^a		
		H	D15	C80-D15-H-M-1 ^a C80-D15-H-M-2 ^a		
			T50	C50	N	D15
		H				C50-D15-H-T50-1 C50-D15-H-T50-2
		T65	C50	N	D15	C50-D15-N-T65-1 C50-D15-N-T65-2
H	C50-D15-H-T65-1 C50-D15-H-T65-2					

^a Smart Strands used for dead end.

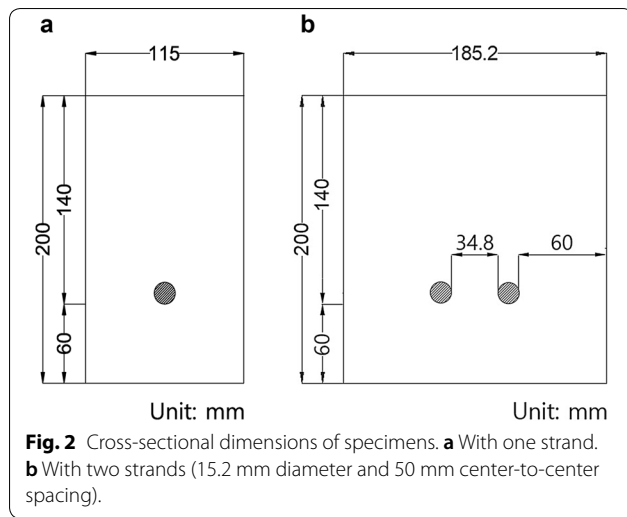
^b Smart Strands used for both cut and dead ends.

ends of a specimen according to previous studies. Confining transverse reinforcements, i.e., stirrups, were not arranged because they did not significantly affect the transfer length (Kim et al. 2016b; Russell and Burns 1996). Table 3 shows the proportion of each level of concrete strength in the concrete mixture, where the fine aggregate is washed sea sand and the coarse aggregate is crushed granite produced in Korea.

Upon release of prestressing tendons by cutting the tendons using flame on one side of the pretensioning bed, the cut end experiences abrupt transfer of prestress, whereas the opposite end (called dead end hereafter) is subject to gradual transfer. These two types of transfer speed can also be regarded as test variables, although they were not included in the identification scheme shown in Fig. 1.

3.2 Test Procedure and Measurement Plan

Figure 3a shows the pretensioning bed consisting of steel frames, the strands tensioned using a mono-strand jack and anchored at the bulk-heads, and wood forms of specimens. Smart Strands were arranged by replacing the corresponding regular strands in the 12 specimens displayed in Table 2, and ERSGs were mounted on the helical wires of strands before tensioning. Load cells were additionally used to measure the prestressing force more accurately, although the force is basically measured at the jack during tensioning. After casting concrete into the forms, the concrete was cured at 65 °C via steam curing for about 2 days. The curing process was accelerated in



this way until the concrete strength exceeded the minimum strength required for the transfer as is often done in a precast plant. Then, after removing the forms, ERSGs for concrete were attached at the concrete surface. Figure 3b shows flame cutting of the strands. All the measurement system was set up in advance before the cutting and the strains of concrete and strands were measured during the transfer of prestressing force into a concrete specimen upon cutting.

Three types of gauges were utilized in this study: ERSGs for concrete, Smart Strands, and ERSGs for strands, represented by CG (concrete gauge), SM (Smart Strand), and SG (strand gauge), respectively, hereafter. Gauge lengths of CG and SG are 60 mm and 5 mm, respectively. DEMEC gauges were not used in this study

because of a wide range of variation and inherent errors in measured data depending on the skill of technicians (Kim et al. 2016b; Park et al. 2012), although they were popular in many studies investigating transfer length as briefly introduced in chapter 2.

The need for the development of Smart Strands has been addressed in previous studies (KICT 2013; Kim et al. 2015, 2019). As the comparative analysis in Fig. 4 shows, the Smart Strand section is almost identical to that of a regular strand measuring 15.2 mm in diameter. In the Smart Strand, the steel core wire of a regular strand is replaced with carbon fiber reinforced polymer (CFRP) wherein a fiber optic sensor with an intended number of fiber Bragg gratings (FBGs) is embedded during the manufacture of the CFRP core wire. Characteristics, advantages, and applications to various engineering fields of fiber optic sensors can be found in previous studies (Bao et al. 2019; Fan et al. 2019; Huang et al. 2019).

The measured wavelength of a reflected light wave at each FBG can be converted to strain at the corresponding point as shown in Eq. (1).

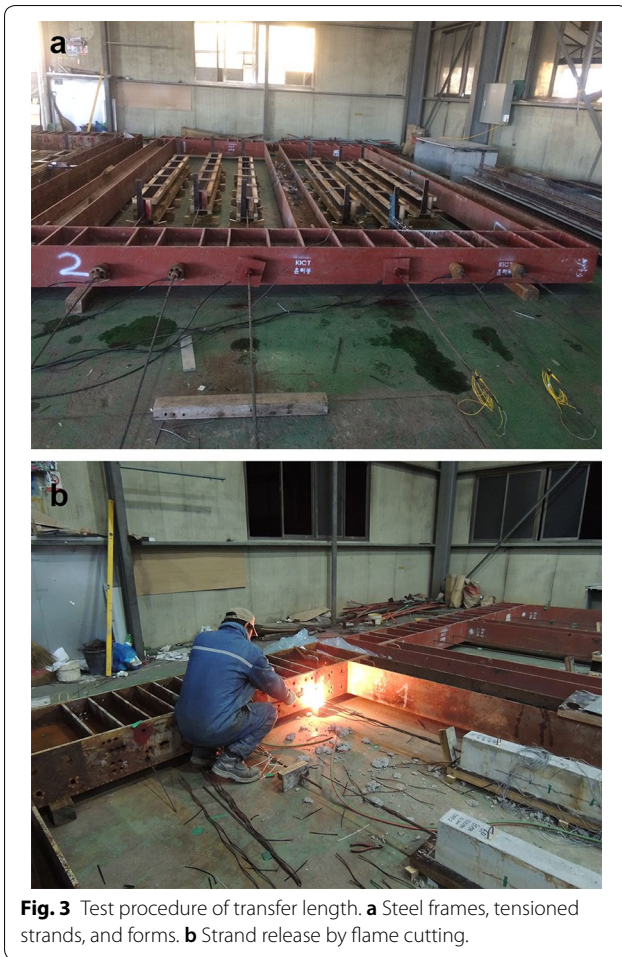
$$\varepsilon = \frac{1}{1 - p_e} \cdot \frac{\Delta\lambda}{\lambda_B} \tag{1}$$

where ε : strain, p_e : photo-elastic coefficient (0.22), $\Delta\lambda = \lambda - \lambda_B$: wavelength shift, λ : measured wavelength, and λ_B : base wavelength at the start of measurement. The advantages of Smart Strand include highly accurate measurement using fiber optic sensors rather than ERSGs, direct measurement of the actual axial strain of a strand, reliable short-term and long-term measurement due to sensor protection, and so forth. Furthermore,

Table 3 Mix proportions of concrete.

f'_c (MPa) ^a	G_{max} (mm) ^b	Air content (%)	Slump (mm)	W/B (%)	S/a (%) ^d	Unit weight (kg/m ³)				AD (B%) ^k	
						W ^e	B ^f	FA ⁱ	CA ^j		
							C ^g	SF ^h			
35	25	3	120	37.5	45	157	440	–	786	959	3.96
50	25	6	120	29.5	43.5	166	563	–	707	936	5.63
80	25	3	500 ^c	27.2	39.9	179	612	68	587	881	8.84

^a Specified compressive strength.
^b Maximum size of coarse aggregate.
^c Slump flow.
^d Sand-to-aggregate volume ratio.
^e Water.
^f Binder.
^g Cement.
^h Silica fume.
ⁱ Fine aggregate (sand).
^j Coarse aggregate.
^k Admixture (water-reducing agent).



the Smart Strand exhibits mechanical properties such as load-strain relationship similar to those of a regular strand (KICT 2013).

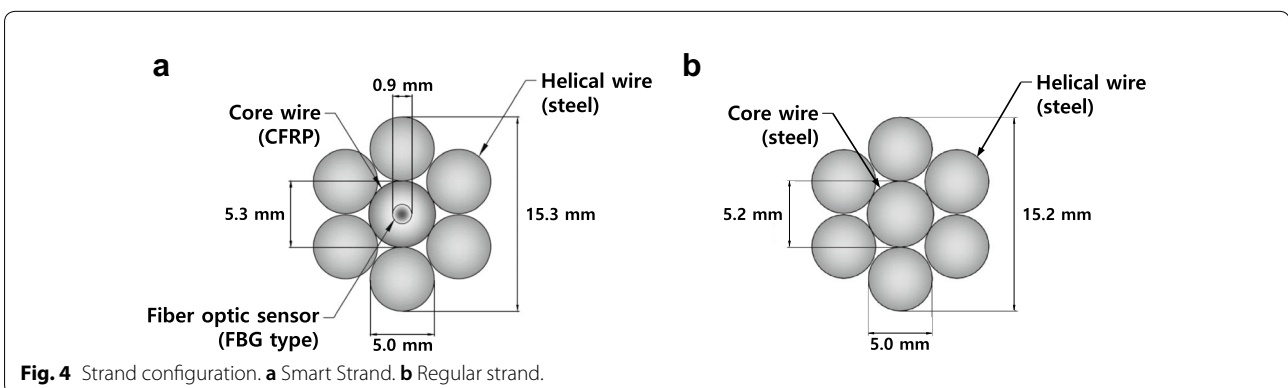
The aforementioned three types of sensors were arranged at both ends of a specimen at a distance ranging between 250 and 1350 mm from the end as shown in Fig. 5. The distance was determined to sufficiently cover the anticipated range of transfer lengths by referring

to the cases discussed in previous studies. A total of 24 CGs were attached to the surface of one side of a specimen with an interval of 100 mm. They were located at the same height as that of the strands to better estimate the transfer length related to strand behavior. On the other hand, SGs were mounted on the helical wires at an interval of 200 mm. Two SGs per measurement point were assigned in opposite directions to the core wire for redundancy because SGs are susceptible to damage at transfer and during casting of the concrete (Russell and Burns 1996). Also, even though the SGs are usually protected by waterproof coating and tape, only waterproof coating was used in this test to reduce the interference with the bond between the strand surface and the surrounding concrete. The Smart Strands were selectively used as presented in Table 2, in which the FBGs show the same interval of 200 mm compared to SGs. Thus, the Smart Strands were applied to the specimens carrying the single strand with 15.2 mm diameter. Among these specimens, those with a concrete strength of 50 MPa contained FBGs at both cut and dead ends, whereas those with 35 MPa or 80 MPa strength displayed FBGs only at the dead end considering that the dead end is more dominant in the long line method usually used for mass production of pretensioned members at a precast concrete plant. Two types of data loggers were used for data acquisition. One was dedicated to measurement of ERSGs and the other was used to measure the data at FBGs.

4 Experimental Results

4.1 Estimation of Transfer Lengths

Transfer length of a pretensioned member can be estimated based on the longitudinal strain distribution in the strand or concrete. The end strain showed approximately linear variation in distribution, and the distance from the end where the strain converges to a nearly constant value can be regarded as the transfer length. The strain distribution also resembles the distribution of bond stress, which is closely related to the transfer length. However, it may be difficult to clearly determine the strain plateau



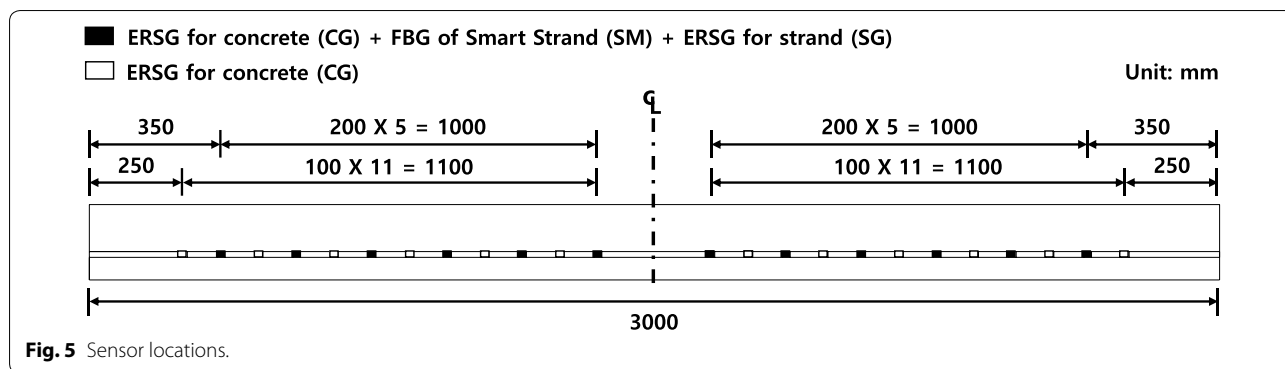


Fig. 5 Sensor locations.

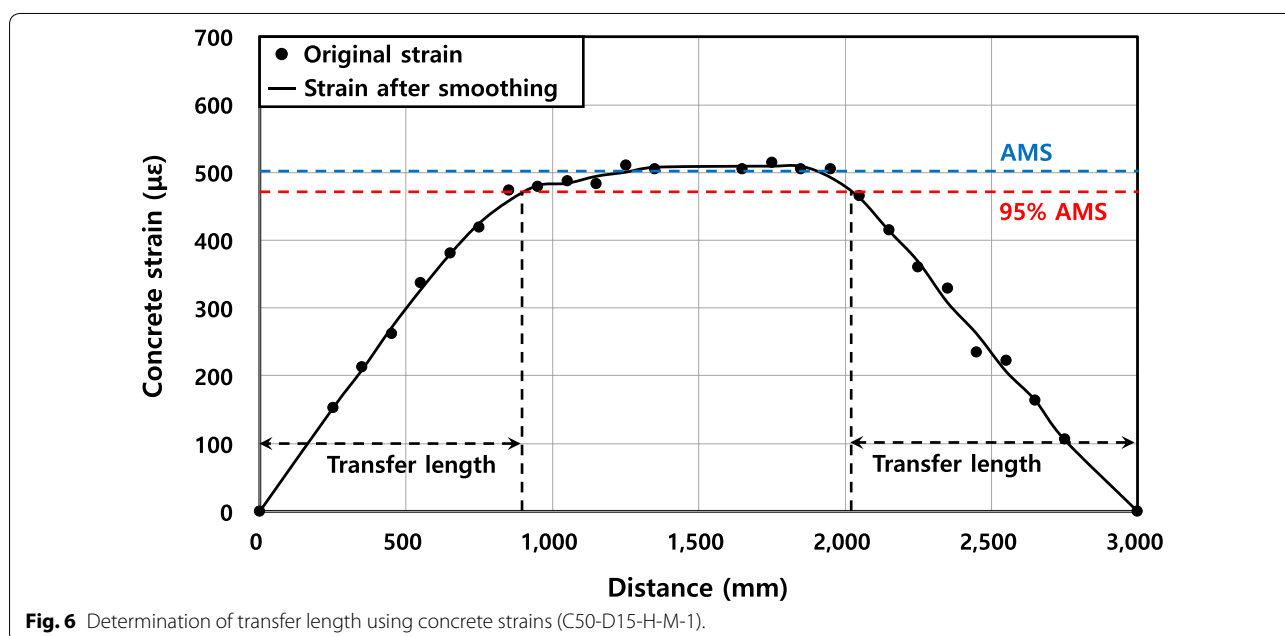


Fig. 6 Determination of transfer length using concrete strains (C50-D15-H-M-1).

with a constant value and the related transfer length because of strain fluctuation. In order to address this issue, the 95% average maximum strain (AMS) method proposed by Russell and Burns (1996) was adopted in this study to determine the transfer length. In the 95% AMS method, the strain distribution plateaued when the rate of increase was lower than 5%. The measured values within the strain plateau were averaged to determine the AMS. A slightly lower value of 95% AMS was used to determine the transfer lengths bilaterally based on the two points of intersection between the 95% AMS line and the distribution curve of strain.

Also, a smoothing technique was introduced for the narrowly-spaced concrete strains obtained by CGs to reduce the anomalies. Toward this end, three adjacent strains were averaged as reported by Russell and Burns (1996). However, this type of smoothing procedure was not applied for the values measured using SMs and

SGs because of the less narrow spacing between these sensors.

Figure 6 presents sample original data measured using CGs together with the smooth curve obtained using the averaging process. It also shows the AMS and 95% AMS and the transfer lengths determined from 95% AMS.

4.2 Results of Transfer Lengths

Figure 7 shows a representative example of strain distribution measured using three types of sensors and the transfer lengths determined from each strain distribution. The concrete strain starts from zero at both ends and increases inward, whereas those of the strands obtained using SMs or SGs display opposite trend because of the shortening strand strain during transfer, as shown in Fig. 7. However, it only represents a form of strain expression and does not distinguish transfer length estimation. Table 4 presents all the transfer lengths

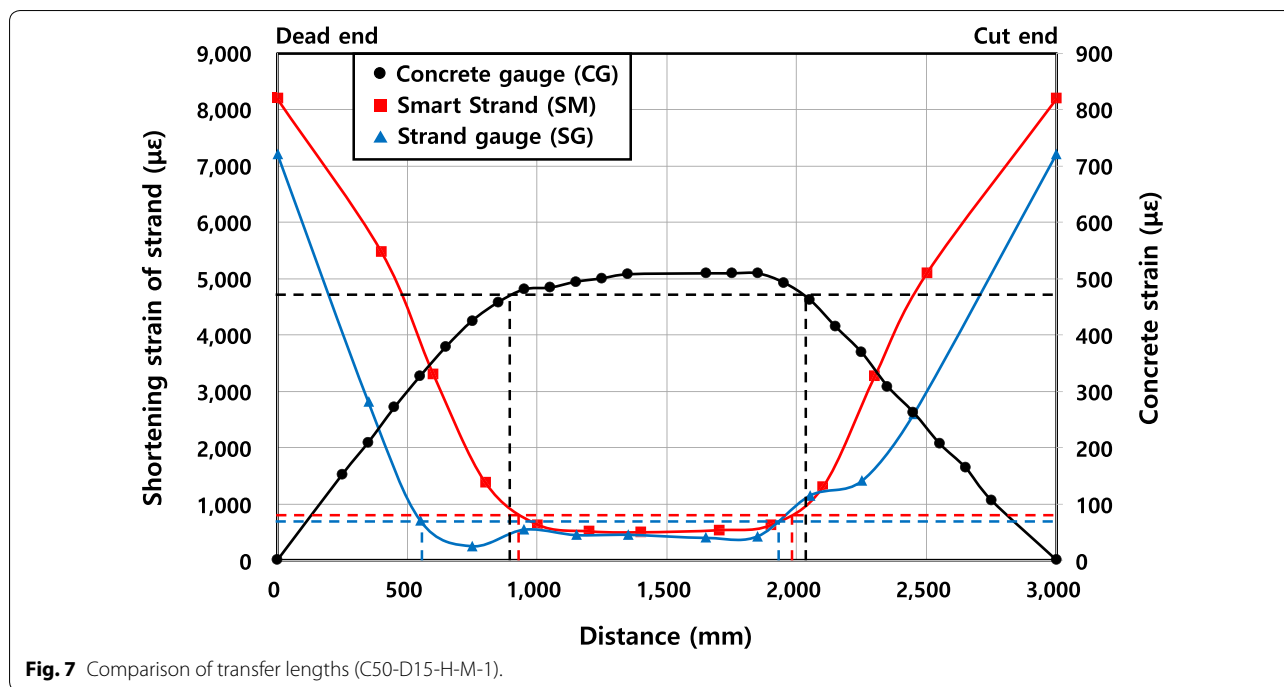


Fig. 7 Comparison of transfer lengths (C50-D15-H-M-1).

obtained from various sensors. The C35-D15-H-M-2 specimen could not be measured due to accidental strand rupture during tensioning. In the specimens included in the C35-D15 series, strains using Smart Strands were obtained at the cut end by changing the initial measurement plan at dead end while accommodating the measurement system. The strains in C80-D15 series using Smart Strands were not available for technical reasons.

4.3 Comparison of Three Types of Sensors

As shown in Fig. 7 and Table 4, the strain distribution and transfer lengths obtained using the three types of sensors differed from one another. Although the strain distribution of concrete has been preferred to other measures for the determination of transfer length (Kim et al. 2016b; Oh and Kim 2000; Park 2015; Russell and Burns 1996) due to the convenient installation and measurement, the results of this study suggest, at least, that the concrete strain may not be the most recommended option to determine the transfer length. According to the original definition of the transfer length as the interaction between a strand and surrounding concrete, it is more reasonable and ideal to rely on strand strain to calculate the transfer length (Russell and Burns 1996). The strains at the strand and concrete surface during the transfer vary because the strains in the strand and the surrounding concrete differ due to the bond-slip behavior (Park 2015). Further, the strains in

the surrounding concrete in contact with the strand and at the corresponding concrete surface cannot be identical due to the non-uniform deformation of a section at transfer.

Based on the C50-D15 series listed in Table 4, the ratio of the transfer lengths measured using SMs to those using CGs (SMs/CGs) ranged from 90 to 104% with an average of 97%. On the other hand, the ratio of the transfer length in terms of SGs/CGs ranged from 59 to 107% with an average of 76%. The strains obtained by Smart Strands are stable and reliable, and therefore, can be regarded as the most desirable measures of transfer length, and the transfer lengths derived from CGs are acceptable when considering SMs/CGs. That is, the concrete strains may still be an effective approach to determine the transfer length, although the transfer lengths derived from the concrete strains were slightly larger than those obtained from the Smart Strands in this study. However, the transfer lengths using SGs varied significantly from those obtained using CGs primarily due to the large fluctuation in strain distribution using SGs. Even though the transfer lengths obtained by SGs were far smaller than those determined using CGs in this study, less reliable data of SGs prevent any generalization. While the protective tape for SGs was intentionally excluded to mitigate the effect on the bond stress as mentioned earlier, the limited protection

Table 4 Results of transfer lengths.

No.	Specimen ID	Transfer length (mm)					
		Concrete gauge (CG)		Smart Strand (SM)		Strand gauge (SG)	
		Cut end	Dead end	Cut end	Dead end	Cut end	Dead end
1	C35-D15-N-M-1	729	623	736	–	730	608
2	C35-D15-N-M-2	838	729	950	–	880	692
3	C35-D15-H-M-1	752	615	734	–	712	701
4	C35-D15-H-M-2	–	–	–	–	–	–
5	C35-D12-N-M-1	416	405	–	–	523	511
6	C35-D12-N-M-2	519	467	–	–	716	539
7	C50-D15-N-M-1	1032	1011	940	914	874	645
8	C50-D15-N-M-2	1187	826	1136	819	889	711
9	C50-D15-H-M-1	986	919	1011	924	1058	545
10	C50-D15-H-M-2	1287	936	1258	977	800	732
11	C50-D12-N-M-1	852	696	–	–	885	511
12	C50-D12-N-M-2	1083	640	–	–	1117	719
13	C80-D15-N-M-1	499	459	–	–	532	521
14	C80-D15-N-M-2	513	349	–	–	505	332
15	C80-D15-H-M-1	691	403	–	–	515	473
16	C80-D15-H-M-2	945	369	–	–	657	327
17	C80-D12-N-M-1	334	248	–	–	332	330
18	C80-D12-N-M-2	361	265	–	–	332	332
19	C50-D15-N-T50-1	841	612	–	–	857	507
20	C50-D15-N-T50-2	849	791	–	–	685	501
21	C50-D15-N-T65-1	813	630	–	–	917	788
22	C50-D15-N-T65-2	1207	846	–	–	905	516
23	C50-D15-H-T50-1	1106	793	–	–	913	876
24	C50-D15-H-T50-2	1315	926	–	–	853	735
25	C50-D15-H-T65-1	1264	768	–	–	1022	596
26	C50-D15-H-T65-2	996	779	–	–	1075	735

of SGs is another source of damage or poor performance at transfer, or during casting and steam curing of concrete. Furthermore, in spite of these measures, the presence of SGs may affect the bond stress and transfer length.

Russell and Burns (1996) mentioned several reasons why the SGs cannot be effectively used for transfer length and these factors coincide with those reported in this study and previous studies (KICT 2013). Although Park et al. (2012) insisted that SGs are a viable option to derive transfer length when they are narrowly spaced at an interval less than 150 mm, the application of SGs for this purpose is still questionable, at least, due to the cumbersome and time-consuming tasks involved and the high sensitivity of measurement affected by workmanship. Consequently, the recently developed Smart Strands were one of the effective options introduced to study transfer lengths.

5 Analysis of Transfer Lengths

Three types of gauges were used to analyze the effect of each test variable on the transfer length. Also, comparisons were made with the various design equations introduced earlier, where the abbreviations of the codes or specifications were as defined in Table 1.

5.1 Effect of Concrete Strength

The effect of concrete strength on the transfer length has been disputed (Russell and Burns 1996). Some studies or provisions suggest that the transfer length was decreased as the concrete strength increased (Han et al. 2019; Kim et al. 2016a), while other studies barely reported a specific relationship (Paul et al. 1963). Figure 8 depicts the study results including the actual concrete strengths at transfer indicated in brackets. The data of mono-strand specimens were only included and averaged in Fig. 8 for consistency. The results did not show a consistent

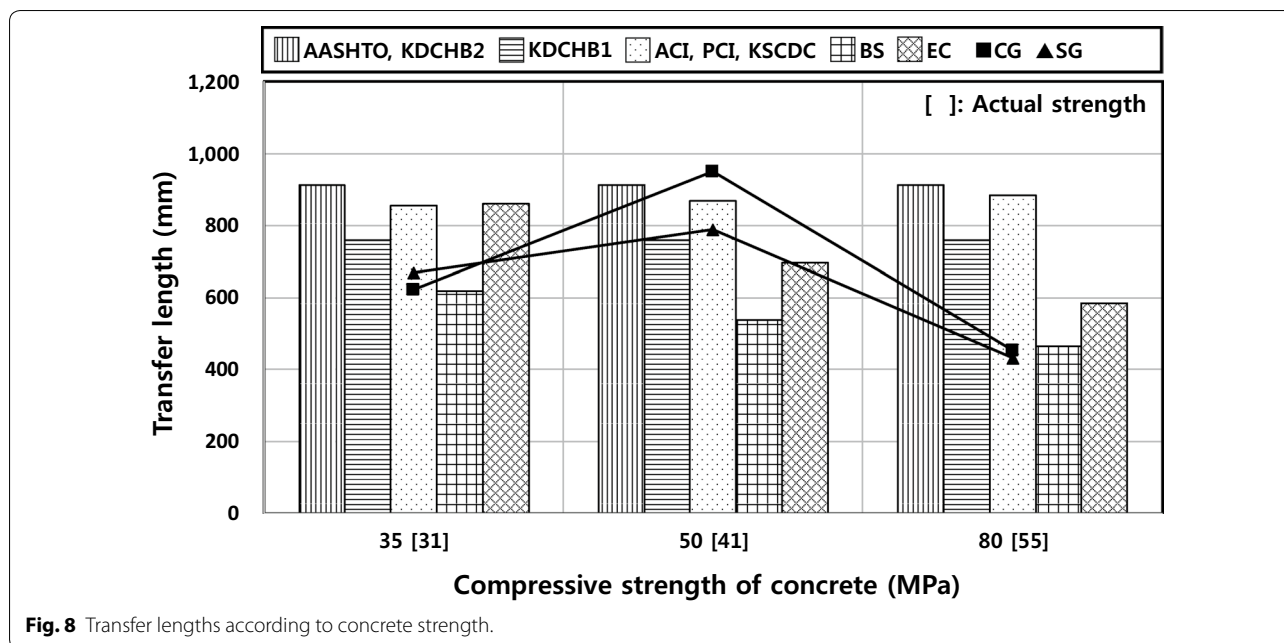


Fig. 8 Transfer lengths according to concrete strength.

decrease with increasing strength. However, if the specimens of 50 MPa are excluded, the test results are similar to BS 8110, which is inversely proportional to the square root of concrete strength.

The concrete strength included in some provisions of transfer length represents bond strength. Although the bond strength is generally increased as the compressive strength increases based on a specific proportional factor incorporated in BS 8110 and Eurocode 2, other provisions in Table 1 ignore strength contribution. The bond strength is known to have a relationship with several factors besides the concrete strength, which can possibly result in an unclear trend with respect to the concrete strength. Referring to ACI 408R-03 (ACI Committee 408 2003), the factors that affect the bond characteristics not only include concrete strength but also the type and quantity of aggregate, slump, admixtures, consolidation even if the scope is limited to concrete properties. Martí-Vargas et al. (2013) concluded that the water-to-cement ratio and the amount of cement also affect the bond behavior of strands. These studies indicate that the transfer length may not simply be defined as a function of concrete strength but may involve various factors related to concrete microstructure. Based on the concrete mix proportions presented in Table 3, the air content in the mixture of 50 MPa was twice that of other two mixtures. Because higher air content induces higher porosity, the bond stress is possibly decreased due to the reduced contact area between the concrete and strand, thereby increasing the transfer length of the mixture of 50 MPa. However, the effect of concrete properties on the transfer

length and its role in design equations requires further investigation using accumulated experimental data.

5.2 Effect of Strand Diameter

The transfer length in ACI 318 shown in Table 1 was determined under the equilibrium conditions of Eq. (2) at the transfer zone between prestressing force and the contact force due to bonding, assuming a constant bond stress. Thus, the transfer length is proportional to the strand diameter as suggested by most parameters including those listed in Table 1.

$$(U_t \Sigma_O) l_t = A_p f_{se} \tag{2}$$

where U_t : transfer bond stress, Σ_O : strand perimeter, l_t : transfer length, A_p : strand cross-sectional area, and f_{se} : effective prestress of strand. Figure 9 shows the results of analysis for the single-strand specimens. The theoretical proportional factor between 12.7 mm- and 15.2 mm-diameter strands is 18%, and that of CGs and SGs was 22% and 16%, respectively, consistent with the theory. Among the provisions, Eurocode 2 showed good agreement with the measured data.

5.3 Effect of Tensile Strength of Strand

As mentioned earlier, about 64% of the ultimate tensile strength was introduced in the strands. According to Eq. (2), the transfer length is proportional to the strand stress included in specific design equations listed in Table 1. Nevertheless, an apparent increase according to the strand stress was not found in single-strand specimens shown in Fig. 10. A few other equations listed

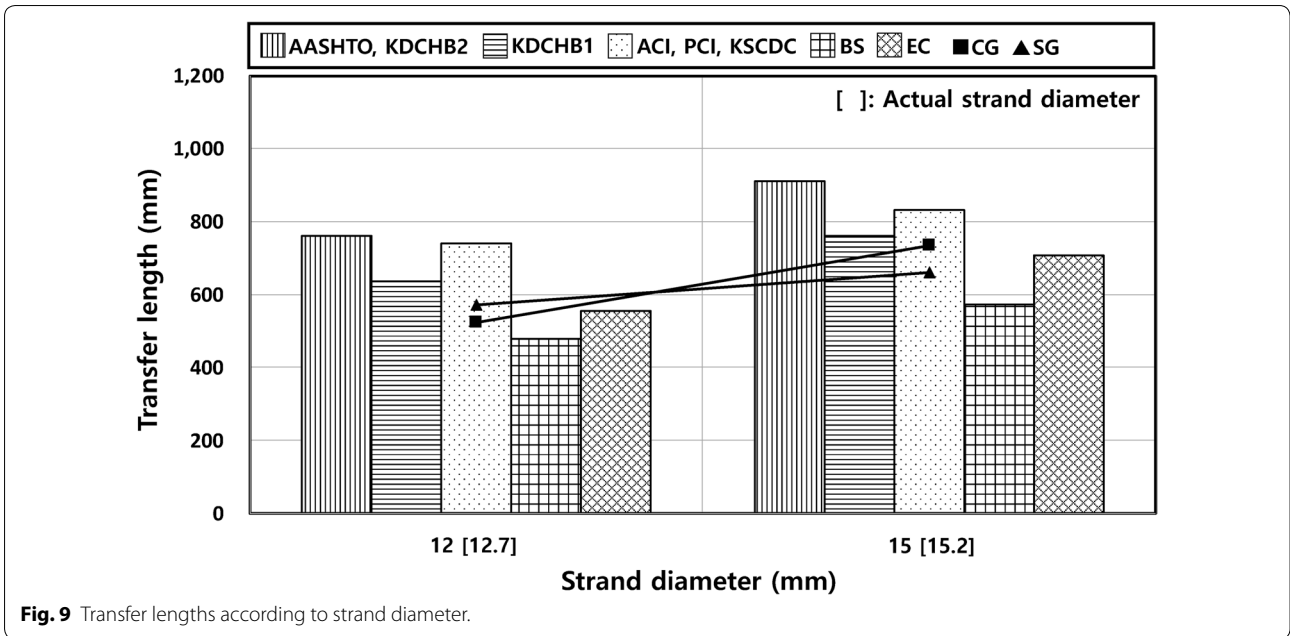


Fig. 9 Transfer lengths according to strand diameter.

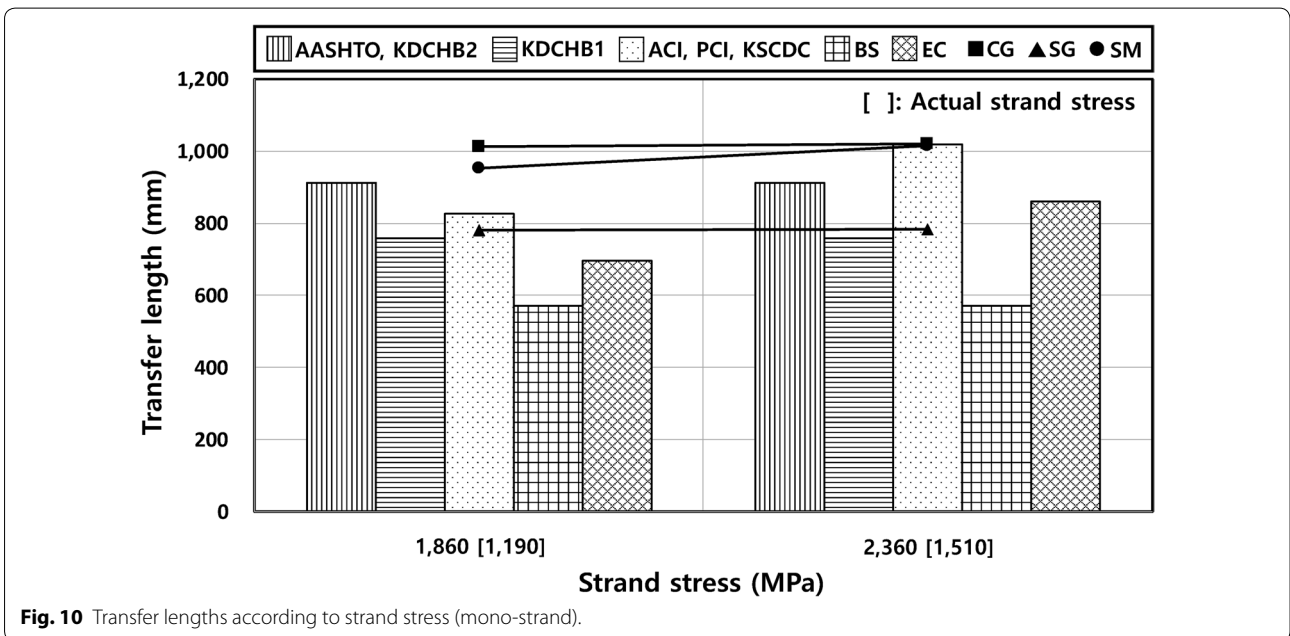
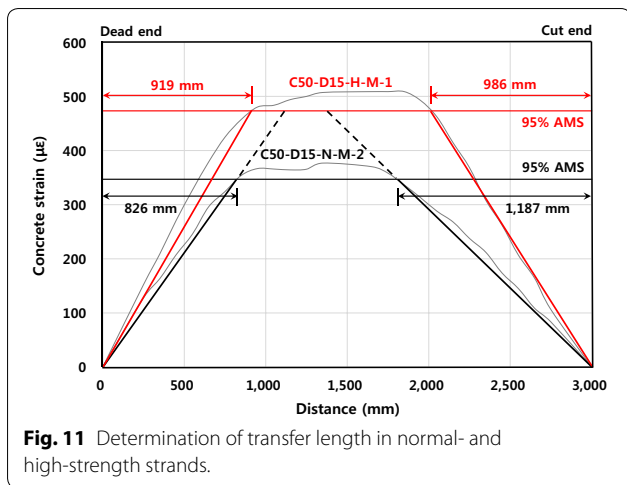


Fig. 10 Transfer lengths according to strand stress (mono-strand).

in Table 1 are independent of strand stress, depending on two perspectives: (1) assumption of specific strand stress in ACI 318 equation; and (2) exclusion of the effect of strand stress. However, due to the large difference depending on gauge types, it was difficult to determine which provision truly estimated the test results.

An attempt was made in this study to elucidate the factors underlying strand stress. Figure 11 demonstrates the strain distribution of concrete and the transfer lengths

determined from two representative specimens under different strand stress, where the strain curves were approximated by straight lines. If the slopes of the lines were identical with each other, the transfer length would be increased in the strand with higher strength as shown by the dashed lines. Judging from the similar figures of two triangles, the transfer length determined from the dashed lines corresponds to the value based on direct proportionality to strand stress. However, the higher



strand stress led to steeper slopes of lines in the transfer zone (24% and 55% steeper in dead and cut ends, respectively, in Fig. 11), resulting in unclear transfer lengths: increase in dead end by 11% and decrease in cut end by 17% from normal- to high-strength strand. This phenomenon can be reasonably addressed by adopting the Hoyer effect. The Hoyer effect is intensified in the higher-strength strand with larger shrinkage strain at transfer, which induces further resistance provided by concrete in addition to the bond stress, resulting in a steeper slope of strain distribution. The proposed explanations provide a more realistic and reasonable basis underlying the effect of strand stress compared with Kim et al. (2016b) who simply suggested the role of Hoyer effect.

However, as seen in Fig. 12 when the double-strands specimens in T50 or T65 series were analyzed distinct from those of single strand, the strand stress consistently affected the transfer length. According to the equations of ACI, PCI, KSCDC, and EC, as the strand stress increases by 27% from normal- to high-strength strand, the transfer length also increases directly by 27%. The increased ratios were 32–34% and 9–10% for the strands spaced at 50 mm and 65 mm, respectively. Therefore, whether or not the transfer length was affected by the strand stress depended significantly upon the strand number and spacing. In particular, the interaction between multiple strands, which are closely spaced and detensioned from the high levels of prestressing force, possibly intensified the slip behavior of strands, resulting in increased transfer length. However, the strand number and spacing have not been included in the predictive equations for transfer length, which prompts the need for further discussion including the role of minimum center-to-center spacing of 45 mm or 50 mm mentioned earlier, especially for high-strength strands.

Even among the equations of ACI, PCI, KSCDC, and EC that reflect the effect of strand stress, it was difficult to determine the accuracy of estimation due to the variation in the measurement.

5.4 Effect of Strand Spacing

The minimum spacing of pretensioned tendons has been introduced for desirable structural behavior at the anchorage in terms of stress distribution and spalling of concrete, and placing of concrete between the tendons

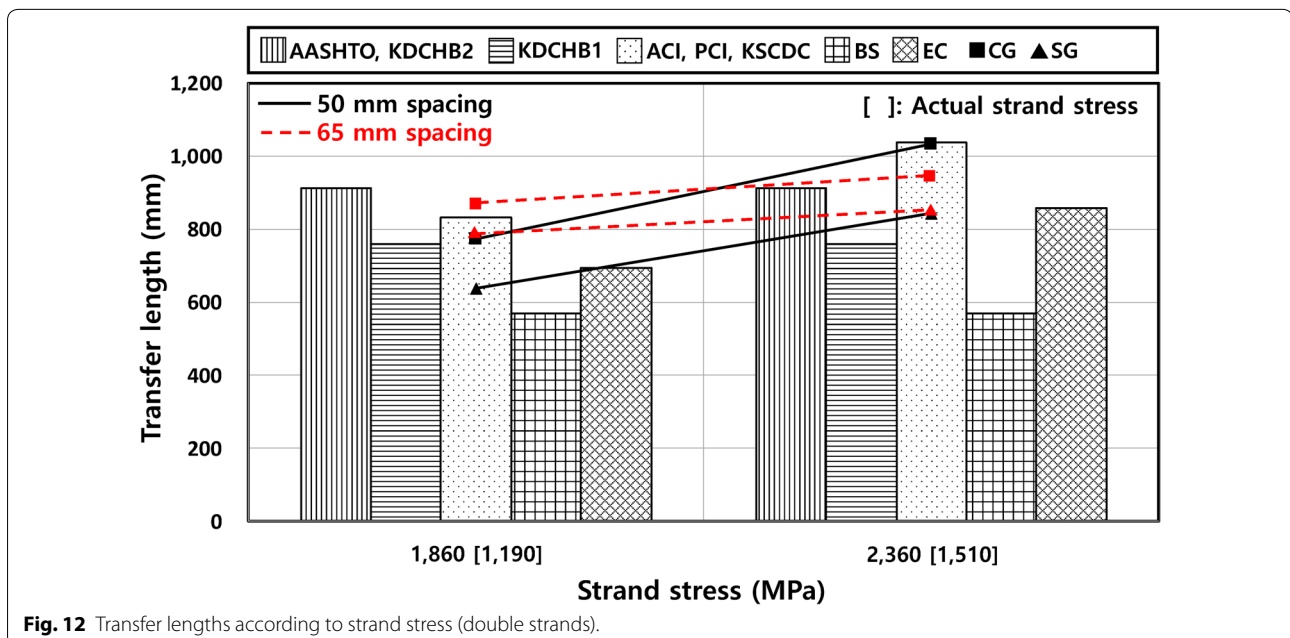


Fig. 12 Transfer lengths according to strand stress (double strands).

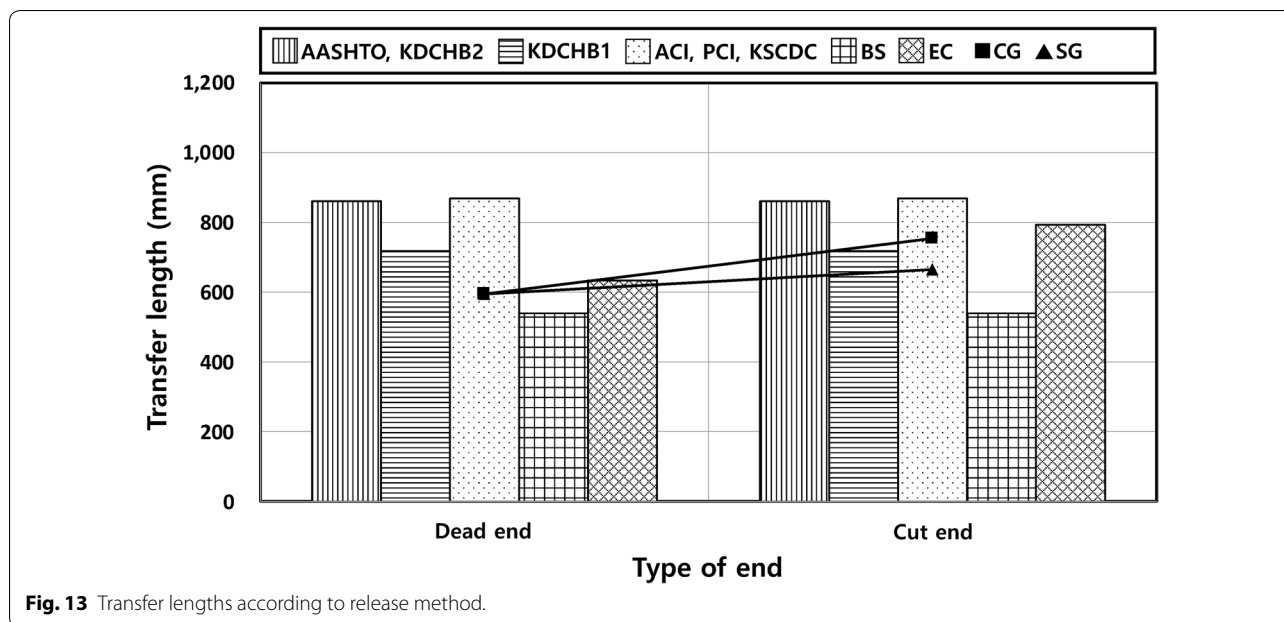


Fig. 13 Transfer lengths according to release method.

(CEN 2004). Oh and Kim (2000) reported that the transfer length was increased as the spacing of normal-strength strands decreased and found that the spacing less than the minimum was still acceptable because the transfer length was within the ACI code value. However, as shown in Fig. 12 this tendency was not apparent in normal-strength strands but was observed only in high-strength strands for the strand spacing of 50 mm and 65 mm which complies with the specifications for minimum spacing. Aside from the transfer length, no spalling or cracking at the ends was observed in the specimens with high-strength strands, which demonstrates the validity of the current minimum spacing based on normal-strength strands for the high-strength strands.

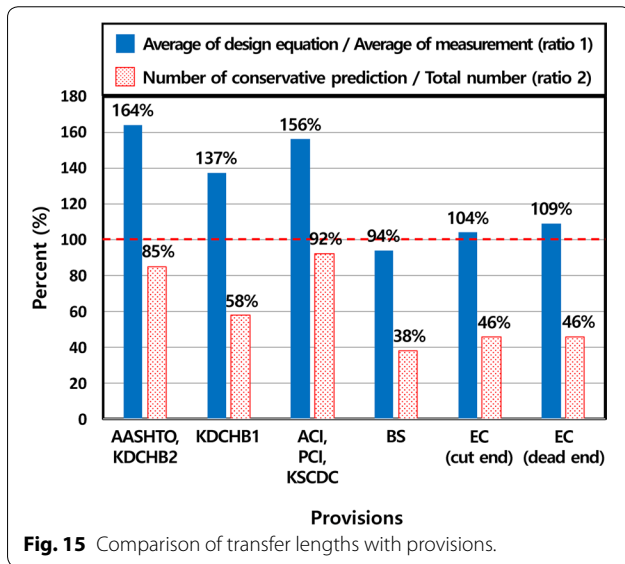
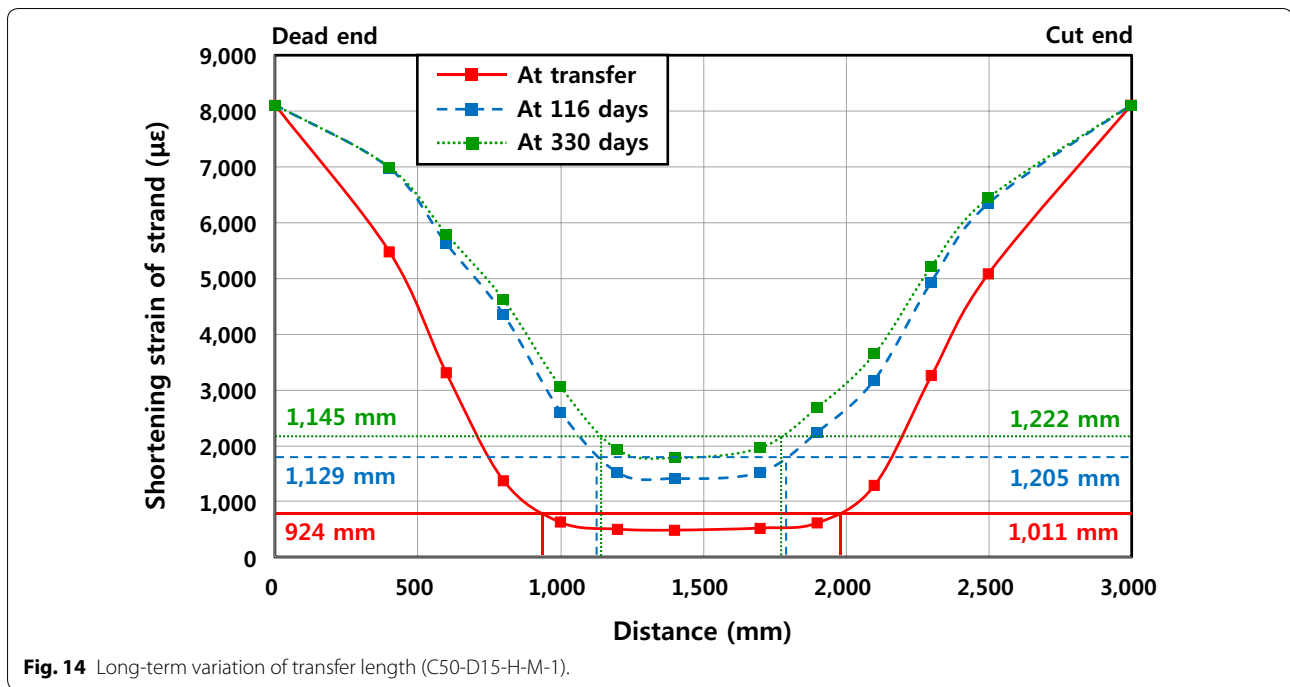
5.5 Effect of Release Method

When an ordinary procedure is used to fabricate the pretensioned members, the cut end is subject to rapid prestress with a strong impact upon cutting while the prestress is introduced gradually at the dead end. Among the predictive equations examined in this study, Eurocode 2 (EC) equation only accounts for the mode of release. When the specimens with mono-strand were analyzed as shown in Fig. 13, CG showed good agreement with the EC equation, with an increased ratio of 27%, although both the CG and SG exhibited increasing transfer length at the cut end. The double-strands specimens showed a further increased ratio as much as 37% due to the magnification of the impact while cutting.

5.6 Long-Term Effect

Long-term variation in transfer length was also investigated in this study using the Smart Strands to ensure a reliable performance for the lifetime of a structure. The durability of the Smart Strand contrasts with the ERSG that has a relatively short guaranteed period of measurement. Figure 14 shows the gradual increase in the transfer length in a representative specimen over a period of 330 days: 21% and 24% increase in cut end and dead end, respectively. A similar trend was observed in other specimens (C50-D15 series) with a Smart Strand: 19% and 23% increase on average in cut end and dead end, respectively, over the same period. The continuous increase in strain magnitude due to creep and shrinkage of concrete did not directly contribute to the increased transfer length, which may be attributed to the relaxation of the Hoyer effect due to the creep of the concrete part supporting the wedge-shaped end of a released strand.

Oh and Kim (2000) reported that the transfer length tended to increase by 5% at 90 days after transfer. However, no longer-term changes were detected due to the foregoing limitations of ERSGs. This study revealed that the degree of long-term increase in transfer length was more significant than was anticipated by Oh and Kim (2000), although this effect was not considered in various provisions. Because the study investigating the long-term effect of transfer length is very rare, further accumulated data are required to generalize the trend. However, it is desirable, at least, that the current provisions are conservative enough to ensure specific margins for the long-term increase in the transfer length.



5.7 Comparison with Provisions

Comparisons were made between the measured data and the provisions listed in Table 1 and the conservativeness of each provision was evaluated in Fig. 15. The transfer lengths derived from CGs were only analyzed for consistency herein. For the provisions that do not vary between the two ends, the data measured at the dead end were compared because of the general prevailing trends.

The design equations specified in AASHTO, KDCHB2, KDCHB1, ACI, PCI, and KSCDC provided a relatively conservative estimation of the transfer length: The average ratio of theoretical values to those obtained via measurement (ratio 1) ranged from 137 to 164%. On the other hand, the equation of BS was slightly less conservative, whereas that of EC resulted in somewhat conservative values. However, the ratio of the number of specimens estimated conservatively to the total number of specimens (ratio 2) was undesirably low at 46% in EC. Therefore, when both ratios were considered, the equations of ACI, PCI, and KSCDC yielded satisfactory results in terms of conservativeness: ratio 1 of 156%; and ratio 2 as high as 92%. Because the ACI, PCI, and KSCDC equations also include the contribution of different prestress levels of a tendon, it can be concluded that the transfer lengths of high-strength strands can reasonably be estimated using these predictive equations.

6 Conclusions

Transfer lengths of pretensioned concrete members were experimentally investigated and compared with several predictive equations in this study. The test variables included diameter, spacing, and stress of strands, concrete strength, speed of transfer, and so forth. In particular, the effect of high-strength strands on the transfer length was analyzed in detail. In addition to conventional strain gauges attached to concrete surface and strands, the Smart Strands recently developed

using fiber optic sensors were applied, and the transfer lengths derived from each sensing technique were compared. Based on the results of this study, the following conclusions can be drawn:

1. The strain distribution and the transfer lengths obtained using three types of sensors differed from one another. It is more reasonable and ideal to rely on the direct strain of strand according to the original meaning of the transfer length related to bond stress. Given that the strains obtained by Smart Strands are most reliable, the transfer lengths derived from the concrete strains were within an acceptable range: the ratio of the transfer lengths measured using Smart Strands to those using concrete gauges ranged from 90 to 104% with an average of 97%. However, the transfer lengths using the strain gauges attached to strands showed significant difference from those obtained using other sensing measures. It was found that this type of strand gauge is difficult to use for the calculation of transfer length due to multiple sources of error and deterioration during fabrication of a member and at transfer.
2. The effect of increased concrete strength on the transfer length did not show a consistent decrease because the bond stress cannot simply be defined as a function of concrete strength, and various factors associated with concrete microstructure affect the bond. In addition to the concrete strength, the differences in air content possibly affected the bond stress in this study. The transfer length was proportional to the strand diameter consistent with theoretical findings and various provisions. As for the release method, the transfer length at cut end was 27% larger than at dead end, which was further magnified to 37% in the double-strands specimens.
3. Although the theoretical hypothesis suggested that the transfer length was proportional to the strand stress as incorporated in specific provisions, no apparent increase was found in the single-strand specimens. This phenomenon can reasonably be explained by the intense Hoyer effect in the higher-strength strands. However, in the double-strands specimens with 50 mm or 65 mm spacing, which exceeds the minimum spacing requirements, the effect of strand stress on transfer length was apparent due to the interaction between multiple strands. Therefore, the effect of strand stress also depends on the number and spacing of strands, although these factors were not incorporated in provisions. The effect of strand spacing on the transfer length was dominant in the specimens with high-strength

strands; however, no spalling or cracking at the ends was observed in these specimens.

4. Long-term measurement using Smart Strands showed gradual increase in the transfer length as much as 19–23% at 330 days after transfer, possibly caused by the relaxation of the Hoyer effect due to the creep of concrete part supporting the wedge-shaped end of a released strand. The provisions need to be conservative enough to ensure adequate margins for long-term increase in the transfer length.
5. Comparisons were made between the transfer lengths experimentally derived and those specified in various provisions. It was difficult to identify the most recommended criterion because the analysis for each test variable resulted in a different optimal provision. Moreover, the differences in strain distribution obtained using different sensing techniques were a hurdle in selecting an appropriate provision. From a conservative point of view, however, the predictive equation of ACI 318 and the Korean structural concrete design code is recommended because the average ratio of theoretical values compared with those measurement values was 156%. This equation provided a conservative estimate of the transfer length in a majority of specimens including those containing high-strength strands.

Acknowledgments

This research was supported by the POSCO Research Grant of 2016. The Smart Strands and steel frames for pretensioning provided by Korea Institute of Civil Engineering and Building Technology are also greatly appreciated.

Authors' contributions

SJJ supervised this project as a principal investigator and wrote the paper. HS and SHK designed, performed, and analyzed the experiments. SYP provided the Smart Strands that were developed in Korea Institute of Civil Engineering and Building Technology. JMY conceived this research project in POSCO. All authors read and approved the final manuscript.

Competing interests

The authors declare that they have no competing interests.

Author details

¹ Department of Civil Systems Engineering, Ajou University, 206, Worldcup-ro, Yeongtong-gu, Suwon-si, Gyeonggi-do 16499, Republic of Korea. ² Department of Civil Engineering, Kyeryong Construction Industrial, 48, Munjeong-ro 48beon-gil, Seo-gu, Daejeon 35262, Republic of Korea. ³ Department of Infrastructure Safety Research, Korea Institute of Civil Engineering and Building Technology, 283, Goyang-daero, Ilsanseo-gu, Goyang-si, Gyeonggi-do 10223, Republic of Korea. ⁴ Department of Civil Engineering, Keimyung University, 1095, Dalgubeol-daero, Dalseo-gu, Daegu 42601, Republic of Korea.

Received: 29 April 2019 Accepted: 26 June 2019

Published online: 15 August 2019

References

ACI Committee 318. (2019). *Building code requirements for structural concrete (ACI 318-19)*. Farmington Hills: American Concrete Institute (ACI).

- ACI Committee 408. (2003). *Bond and development of straight reinforcing bars in tension (ACI 408R-03)*. Farmington Hills: American Concrete Institute (ACI).
- American Association of State Highway and Transportation Officials (AASHTO). (2017). *AASHTO LRFD bridge design specifications* (8th ed.). Washington, D.C.: AASHTO.
- American Society for Testing and Materials (ASTM). (2018). *Standard specification for low-relaxation, seven-wire strand for prestressed concrete (ASTM A416/A416M-18)*. West Conshohocken: ASTM.
- Bao, Y., Huang, Y., Hoehler, M. S., & Chen, G. (2019). Review of fiber optic sensors for structural fire engineering. *Sensors*, *19*, 877.
- Briere, V., Harries, K. A., Kasan, J., & Hager, C. (2013). Dilation behavior of seven-wire prestressing strand—The Hoyer effect. *Constr Build Mater*, *40*, 650–658.
- British Standards Institution (BSI). (1997). *Structural use of concrete (BS 8110)*. London: BSI.
- European Committee for Standardization (CEN). (2004). *Design of concrete structures (Eurocode 2)*. Brussels: CEN.
- Fan, L., Bao, Y., Meng, W., & Chen, G. (2019). In-situ monitoring of corrosion-induced expansion and mass loss of steel bar in steel fiber reinforced concrete using a distributed fiber optic sensor. *Compos B Eng*, *165*, 679–689.
- Han, S. J., Park, M. K., Chung, J. H., Kim, K. S., & Seo, S. Y. (2019). Experimental study on transfer length of prestressing strands in UHPC members. *J Korea Concr Inst*, *31*(1), 41–48.
- Hayek, C., & Kang, T. H. K. (2017). Elongation tolerance for short tendons in post-tensioned building structures. *ACI Struct J*, *114*(4), 795–802.
- Huang, Y., Bao, Y., Chen, G., & Zhou, Z. (2019). A constrained cylinder model of strain transfer for packaged fiber Bragg grating sensors embedded in inelastic medium. *Struct Contr Health Monit*, *26*, 2335.
- Huang, Y., & Kang, T. H. K. (2018). Modeling of sliding behavior of unbonded tendons in post-tensioned concrete members. *ACI Struct J*, *115*(4), 1153–1164.
- Kim, M. S., Han, S. J., Cho, H. C., Oh, J. Y., & Kim, K. S. (2016a). Prediction of transfer lengths in pretensioned concrete members using neuro-fuzzy system. *J Korea Concr Inst*, *28*(6), 723–731.
- Kim, S. T., Park, Y. H., Park, S. Y., Cho, K. H., & Cho, J. R. (2015). A sensor-type PC strand with an embedded FBG sensor for monitoring prestress forces. *Sensors*, *15*, 1060–1070.
- Kim, S. H., Park, S. Y., Park, Y. H., & Jeon, S. J. (2019). Friction characteristics of post-tensioning tendons in full-scale structures. *Eng Struct*, *183*, 389–397.
- Kim, J. K., Yang, J. M., & Yim, H. J. (2016b). Experimental evaluation of transfer length in pretensioned concrete beams using 2,400-MPa prestressed strands. *J Struct Eng*, *142*(11), 04016088.
- Korea Concrete Institute (KCI). (2012). *Structural concrete design code*. Seoul: KCI.
- Korea Institute of Civil Engineering and Building Technology (KICT). (2013). *Development of smart prestressing and monitoring technologies for prestressed concrete bridges, KICT 2013-167*. Goyang-si: KICT.
- Korea Road and Transportation Association (KRTA). (2010). *Design code for highway bridges*. Seoul: KRTA.
- Korea Road and Transportation Association (KRTA). (2015). *Design code for highway bridges (Limit state design)*. Seoul: KRTA.
- Korean Agency for Technology and Standards (KATS). (2018). *Uncoated stress-relieved steel wires and strands for prestressed concrete (KS D 7002)*. Seoul: Korean Standards Association (KSA).
- Martí-Vargas, J. R., García-Taengua, E., & Serna, P. (2013). Influence of concrete composition on anchorage bond behavior of prestressing reinforcement. *Constr Build Mater*, *48*, 1156–1164.
- Oh, B. H., & Kim, E. S. (2000). Realistic evaluation of transfer lengths in pretensioned, prestressed concrete members. *ACI Struct J*, *97*(6), 821–830.
- Park, H. (2015). *Behavior and analysis of transfer zone in pretensioned prestressed concrete members*. Ph.D. Dissertation, Seoul National University, Seoul.
- Park, H., Din, Z. U., & Cho, J. Y. (2012). Methodological aspects in measurement of strand transfer length in pretensioned concrete. *ACI Struct J*, *109*(5), 625–633.
- Paul, H. K., Robert, W. L., & Mark, A. M. (1963). Influence of concrete strength on strand transfer length. *PCI J*, *8*(2), 47–67.
- Precast/Prestressed Concrete Institute (PCI). (2017). *PCI design handbook: Precast and prestressed concrete* (8th ed.), MNL-120-17. Chicago: PCI.
- Russell, B. W., & Burns, N. H. (1996). Measured transfer lengths of 0.5 and 0.6 in. strands in pretensioned concrete. *PCI J*, *41*(5), 44–65.
- The International Federation for Structural Concrete (fib). (2013). *fib model code for concrete structures 2010*. Lausanne: fib.

Publisher's Note

Springer Nature remains neutral with regard to jurisdictional claims in published maps and institutional affiliations.

Submit your manuscript to a SpringerOpen® journal and benefit from:

- Convenient online submission
- Rigorous peer review
- Open access: articles freely available online
- High visibility within the field
- Retaining the copyright to your article

Submit your next manuscript at ► [springeropen.com](https://www.springeropen.com)